

The RadFxSat Mission to Study Radiation Effects on Advanced Nanoelectronics

Brian D. Sierawski, Rebekah A. Austin, James M. Trippe[†], Kevin M. Warren,
 Andrew L. Sternberg, Robert A. Reed, Robert A. Weller
 Vanderbilt University
 1025 16th Ave. S., Suite 200, Nashville, TN 37212; 615-343-9833
 brian.sierawski@vanderbilt.edu

Eric Skoog, Gerald W. Buxton, III, W. Burns Fisher, Robert Davis, Christopher E. Thompson
 Radio Amateur Satellite Corporation (AMSAT)
 10605 Concord St, #304, Kensington, MD 20895 USA; 301-822-4376
 info@amsat.org

ABSTRACT

The RadFxSat mission was launched on November 18, 2017 with the Joint Polar Satellite System-1 (JPSS-1) under the NASA ELaNa XIV initiative. RadFxSat, now designated at AO-91, is an AMSAT Fox bus carrying a Vanderbilt University radiation effects payload. Embedded in the sub-audible range of voice transmissions are the telemetry conveying the status of the spacecraft and payload. Since launch, hundreds of amateur radio operators have submitted thousands of telemetry packets. These data can be retrieved using AMSAT's FoxTelem software and are being used by researchers to measure the effects of ionizing radiation on modern commercial electronics.

MISSION DESCRIPTION

In recent years, a number of investigators have discovered that very advanced (scaled) memories are susceptible to data corruption due to direct ionization (as opposed to indirect) from protons.¹⁻⁵ This process of charge generation is typically not considered in classical microelectronic error rate estimates. Proton-rich environments such as low-Earth orbit and near-Earth solar particle events could drive error rates beyond expected or acceptable levels. The relative contribution of proton direct ionization to the total error rate remains unresolved. RadFxSat was designed as part of a campaign to quantify error rates in advanced microelectronics and evaluate radiation modeling and prediction methods. The mission was launched on November 18, 2017 and is still operating. RadFxSat is currently in an 815 km apogee, 453 km perigee orbit with 97.7° inclination and 200° argument of perigee.

RADIATION EFFECTS IN ELECTONICS

Ionizing radiation can have a variety of effects on spacecraft electronics. The effects may be destructive or degrading. They may also be permanent or transient. In this paper, we will focus on one type of effect which is non-destructive, transient, and random in nature. Single event effects (SEE) occur when a particle strikes an electronic device having a measurable impact on the operation. This contrast to cumulative effects, such as total ionizing dose or displacement damage, makes SEE

a constant threat to reliability and survivability from the beginning of a mission until the end.

Corruption of data stored in a memory component is a subclass of SEE known as single event upset (SEU). These events occur because of the bistable nature of charge storage devices like a static random access memory (SRAM). Each bit of data in the integrated chip is susceptible to flip if sufficient charge is promptly introduced in its vicinity. The threshold for a bit flip is known as the critical charge. The industry trend in integrated circuits has been scaling to increase transistor density and concurrently decreasing operating voltages to reduce power. The side effect has been the reduction of critical charge thresholds. Nanoelectronics, or process technologies with physical features on the order of several nanometers, have critical charges on the order of femtocoulombs. The reduction has made memory devices more susceptible corruption in radiations environments.

Single particles are capable of causing other single event effects including latchup, functional interrupts, as well as gate rupture and burnout in power devices. In integrated circuits, single event latchup (SEL) may be destructive. This run-away high-current condition overheats and frequently damages electrical pathways. Once latchup has occurred, the only relief is to remove electrical power from the component to break the feedback. Unfortunately, even after a successful power cycle, latent damage may be hiding within the

[†]James M. Trippe was with Vanderbilt University. He is now with Sandia National Laboratories.

component. Single event functional interrupts (SEFI) are another type of disruption to the nominal operation of microelectronics but are associated with corruption of control logic rather than an electrical dysfunction.

Charge generation from ionizing radiation is introduced through direct and indirect processes. In direct ionization, the primary charged particle loses energy through electronic collisions along its trajectory. This is known as the linear energy transfer (LET) of the particle and is typically normalized to material density to have units of MeV-cm²/mg. Ionized particles with larger atomic mass (really higher charge states) will result in larger LET. The energy loss is also energy dependent; the highest rate of energy loss is near the particle's end of range. For reference, ions in the space environment can reach as high as 100 MeV-cm²/mg in silicon. Iron, a dominant component of the LET spectrum, has a maximum of 26 MeV-cm²/mg in silicon. Direct ionization typically dominates ion-induced single event mechanisms. The process is naturally directional, following the trajectory of the ion. Therefore electronics, because of internal structures, tend to exhibit angular dependence on the probability of single event effects. Sensitive volume models have been developed around this premise.⁶

Protons, however, have a maximum LET of 0.5 MeV-cm²/mg in silicon at their end of the range. At higher energies, charge generated from electronic stopping is negligible. At energies above a few MeV, protons ionize through indirect processes. Coulombic and nuclear scatters within a component result in short-range recoils. Nuclear fragmentation generates secondary products, commonly through interactions with silicon and oxygen atoms because of their abundance in electronics. Both recoils and secondary products have larger atomic numbers than the primary proton and less energy. As a result, the secondary particles "indirectly" deposit a significant portion of the primary particle's energy. The direction of secondary production is largely isotropic so proton single event effects typically do not exhibit angular dependence. The necessary nuclear interaction reduces the probability of occurrence.

Two approaches have developed to independently assess ion-induced and proton-induced single event effects. Unfortunately, the reduction of critical charge thresholds below a few femtocoulomb introduces the direct ionization process into proton-induced SEU. If ignored, missions risk unexpectedly high error rates.

MITIGATING AND PREDICTING SEE

In space, ionizing radiation capable of causing single event effects originates from the galactic cosmic ray

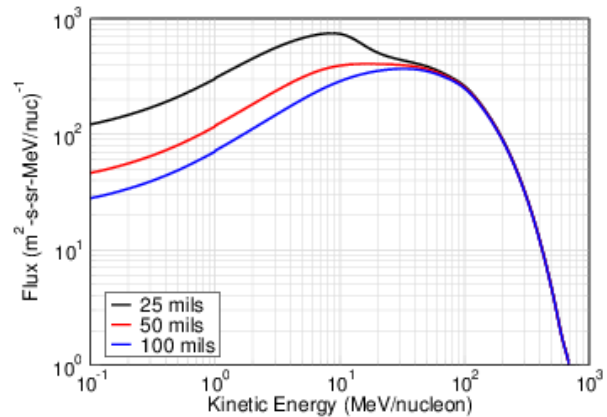
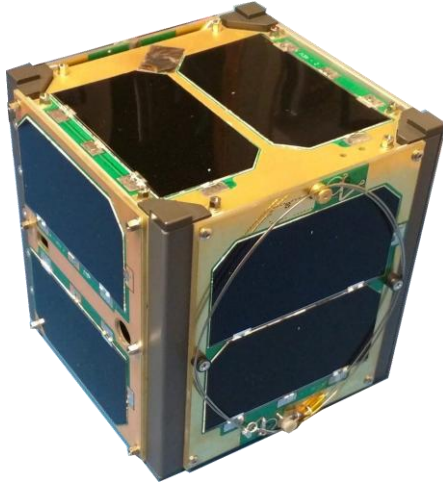


Figure 1: Differential trapped proton spectra for AO-91 with three aluminum shielding thicknesses

background, planetary radiation belts, or solar particle events. The environments differ in the composition of particle species, energies, flux, and even variability. However, the random arrival of a single particle that can cause impacts to the operation of a circuit means that electronics cause experience an anomaly at any point in the mission.

The space radiation environment and its effects are fairly well known today. In fact, the aerospace community has developed ways to address these issues. One hardening strategy is the simple solution of radiation shielding. While this approach can be very effective for low-energy particles, it becomes less useful for the higher energy portion of the environment. To eliminate the remaining risk, the traditional approach has been to use electronic parts that are intentionally hardened to the space environment by design or technology selection. High-budget missions have the luxury of funding and using radiation hardened devices when required. This part selection can be very limited and costly for amateur or low-cost missions. As a result, commercial-off-the-shelf (COTS) electronics are appealing to designers as an avenue to reduce mass, volume, power, and ultimately the cost of launching and operating the satellite. In some cases, automotive or even commercial-grade electronics may prove sufficient.

Therefore we are left with addressing the questions of how severe are the radiation effects and how often will they happen. The radiation hardness assurance process must make predictions of on-orbit part performance based on information obtained on the ground. This typically involves the use of an irradiator or particle accelerator. However both have limitations. A handful of results from ground-based tests using a limited set of particle energies, ranges, and angles must be extrapolated to the full environment of space using models.



**Figure 2: RadFxCubeSat (AO-91) cubesat
(Courtesy of AMSAT)**



**Figure 3: RadFxCubeSat (AO-91) CAD Model
(Courtesy of AMSAT)**

Cosmic Ray Effects on Microelectronics (CREME96)⁶ has been used for over 20 years to assess single events. The suite consists of models for calculating the on-orbit radiation environment including trapped protons, the effects of geomagnetic shielding, solar particle events, and galactic cosmic rays. Simple shielding transport and proton dose calculations can be included. Further, for microelectronics with ground test data, single event rate calculations can be performed.

Figure 1 shows the differential energy spectrum of the trapped proton environment of RadFxCubeSat computed by CREME96 under solar minimum and geomagnetic quiet conditions. Three aluminum shielding thicknesses were evaluated to demonstrate the effect on the incident environment. In RadFxCubeSat, the payload is shielded by a solar panel in the positive Z direction and the spacecraft bus in the negative Z direction. Near 1 MeV, protons have sufficient energy to penetrate component packaging and cause single event upsets.

SPACECRAFT OVERVIEW

RadFxCubeSat was developed as a collaboration between Vanderbilt University and the Radio Amateur Satellite Corporation (AMSAT). This CubeSat is the second design in the AMSAT Fox Project. The first collaboration was the AO-85 CubeSat.⁷ The Fox project pursued a path to put ham radio transponders into space and at the same time provide university partners with a satellite bus for space-based research.⁸ Students and faculty at Vanderbilt University provided the radiation effects experimental payload for integration by AMSAT into the full avionics stack.

RadFxCubeSat, also known as Fox-1B, is shown in Figure 2 with a CAD rendering of the printed circuit board stack

in Figure 3. The avionics stack, from top to bottom, is listed in Table 1. The satellite utilizes six solar panels with two Spectrolab Ultra Triple Junction cells per panel. Each panel supplies current to six maximum power point trackers (MPPT) on the power board designed by Rochester Institute of Technology. The battery card includes six NiCad cells providing a nominal 3.6 V. The Internal Housekeeping Unit (IHU) executes commands from ground control, interfaces with the science payload, collects the system telemetry, and sends the telemetry as sub-audible FSK to the radio. This board is built with an ST Microelectronics STM32L running FreeRTOS. The RF Rx card provides audio to the IHU and RF Tx. is connected to a 70 cm whip antenna. The RF Tx card provides audio processing using inputs from the RF Rx and IHU and transmits with a 2 meter antenna. The structure provides passive attitude control with bar magnets and hysteresis rods on the battery card for damping. This aligns the satellite's z-axis with the Earth's magnetic field.

Table 1: RadFxCubeSat Avionics Stack

Board	Function
REM4	Radiation Experiment (0.85V)
REM3	Radiation Experiment (0.5V)
REM2	Radiation Experiment (0.5V)
VUC	Vanderbilt University Controller
BATT	Battery Card
MPPT	Maximum Power Point Tracker
IHU	Internal Housekeeping Unit
RF Rx	FM receiver
RF Tx	FM transmitter

EXPERIMENT DESIGN

The REM experiment was designed to monitor single event effects in a 28 nm SRAM. The memory is a test chip provided in-kind by Broadcom Corporation and can be seen as the large package in the bottom image of Figure 4. The limited space available on the printed circuit board dictated that the memory be attached to the back side where as the majority of components reside on the front. The memory, like the other components, was not designed to operate in space. The results, however, teach us about modeling radiation effects in commercial-off-the-shelf components. On-orbit single event data are normalized, but should not be taken as an indication of terrestrial reliability as the environments have significant differences. Further, the experiment is designed in ways to gather statistically significant numbers of events necessary for modeling. For example, no error detection and correction methods are applied and the memories can be operated at reduced bias.

The SRAM is used only as the device under test and serves no functional purpose within the satellite. The experiment proceeds by initializing the entire memory to a known data pattern. Then the memory is left to store the data for five minutes. After this period of exposure to the natural radiation environment, the memory is scanned for bit errors. Each instance of an error is tallied and recorded within an off-chip counter. In this way the accumulated error count is recorded and eventually transmitted reducing the need to maintain a history or continuously monitor errors. In addition to the total error count, registers recording the total livetime are incremented. The ratio of the error counts and livetime yield the device error rate. An general, the device error rate is dependent on the number of bits exposed, which is known, but unpublished. After the scan is complete, the SRAM is reinitialized and prepared to conduct another exposure.

Nominal operation for the SRAM is between 0.9 and 1.1V. However, the design is capable of lowering the core voltage as low as 0.3 V to reduce static power consumption and still retaining data. During each exposure the core voltage is set to either 0.5 V or 0.85 V. Each bias condition utilizes a different set of error and livetime registers.

Each experiment is controlled by a Microchip PIC24FJ microcontroller. Each microcontroller on the RadFxSat payload runs experiment software adapted for its particular board. The software is built with FreeRTOS tasks. The microcontroller is responsible for conducting the experiment, reading and writing the SRAM, signaling the remaining components providing the adjustable bias and providing a telemetry string to the RadFxSat flight computer for transmission to the

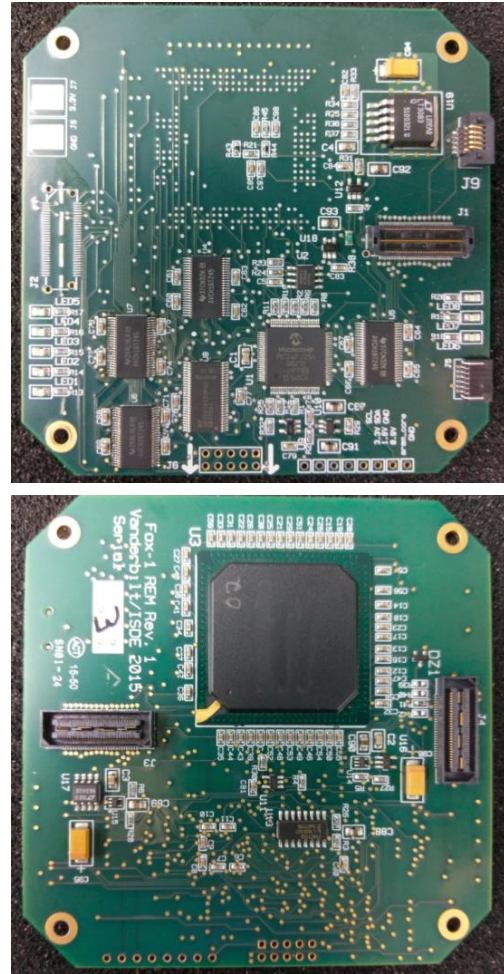


Figure 4: Front-side (top) and back-side (bottom) of 28 nm SRAM board on RadFxSat.

ground. Each call to the FreeRTOS task evaluates a transition in a software state machine. The registers of this state machine are stored off-chip in a non-volatile FRAM which was demonstrated to be proton-induced single event tolerant. In this way, the microcontroller may experience single event effects and even reset without interruption to the experiment data. Although computation and data must eventually reside in the microcontroller, we limit its use to local variables which quickly go out of scope and prohibit global variables that could adversely affect the experiment operation. Further, all control registers are treated as volatile in the sense that the code may not assume flags have remained set between function calls, etc.

A functional interrupt within the microcontroller resulting in failure to progress will be cleared by a hardware watchdog timer within two seconds. Peripheral components are power cycled by the microcontroller if they fail to respond. Also, all commercial components should be suspected to be

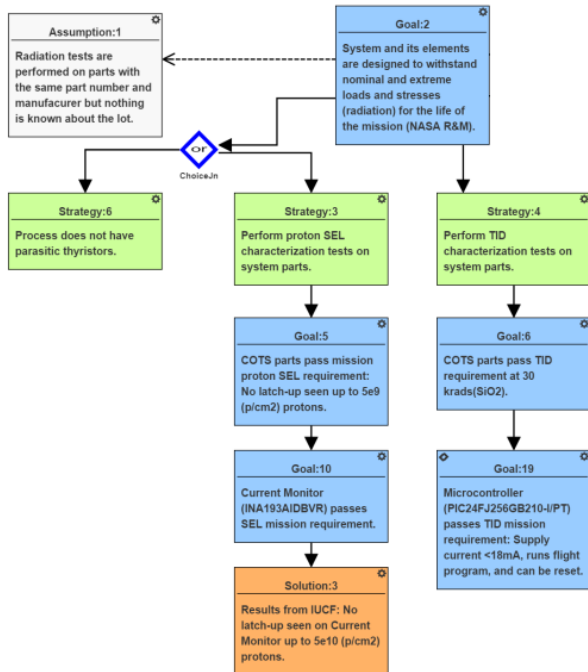


Figure 5: Partial assurance case used to document and review the radiation hardness assurance of the REM experiment

vulnerable to single event latchup unless demonstrated otherwise. As mentioned previous, latchup is a potentially destructive event. Voltage regulators and current limiting is implemented separately for the memory and all other components. Similar components had been previously demonstrated to be proton single event tolerant. All components were screened for total ionizing dose. A complete description of the hardness assurance was previously published.⁹

Further, an assurance case was constructed at the component level for the radiation reliability of the REM experiment.^{10,11} An assurance case is a graphical argument amenable to model based systems engineering that allows one to make a qualitative argument. This approach allowed for documentation and review of part test results and system mitigation approaches. The argument was based on the objectives outlined in NASA STD 8729.1A.¹² The assurance case focused on radiation effects including total ionizing dose screening, detection and recovery from single event latchup, and restart following single event functional interrupts. A complete assurance case includes a series of interconnected objectives, strategies, assumptions, and evidence. A portion of the assurance case is shown in Figure 5. For the REM experiment, where reliability approaches include the system design and not radiation hardened parts, the assurance case provides an effective format to evaluate risk.

PAYLOAD CONFIGURATION

The experiment payload on RadFxBat is called Phoenix. This consists of three REM boards and a Vanderbilt University Controller (VUC) to coordinate the operations between experiments, provide power, and communicate with the bus. Each experiment is configured to run the SRAM at a different bias condition. In this case, two were selected to run at 0.5V because of the primary objective of characterizing low critical charge operation. The payload stack is shown as the top four boards in Figure 3. The exterior panels are omitted. From top to bottom are the REM4 (0.85V), REM3 (0.5V), REM2 (0.5V), and VUC.

Late in the development process it was determined that running all three experiment boards would exceed the payload power budget. Attempts to reduced board-level power consumption were insufficient. The solution was to use the VUC to cycle power between experiments allowing one to run while the other two remain powered off. Provisions were included to ensure the VUC switched between the experiments after several days of operation. This allows each experiment to effectively average its results over multiple orbits. At the same time, experiments are not run so long as to experience large precession in the orbit.

LESSONS LEARNED

Beyond the required shock and vibration tests, we have found temperature testing boards to be good practice. Thermal tests of the boards and the integrated system were completed over a temperature range of -55°C to 85°C using a TestEquity 140 temperature chamber. At elevated temperatures, the payload static power increased as expected. However, a number of issues were identified with power monitoring and restart circuitry at the temperature extremes and even within nominal on-orbit temperatures (~ 0 to -10°C). In particular, at cold temperatures, certain components in the system were found to continuously restart due to the unintentional combination of parameters in the SEL management circuits and inrush current properties of several of the components. The cold temperature enhancement of switching speeds produced currents comparable with trigger levels designed to mitigate anomalous behaviors. The issues were resolved through a design modification and the system performed as designed over the full temperature range.

FOXTELEM

The Fox series of Cubesats have a FoxTelem software package to demodulate, store, and analyze telemetry.¹³ The software is freely available for download from <https://www.amsat.org/foxtelem-software-for-windows-mac-linux/> The decoder is implemented in Java therefore can be used on Windows, Mac & Linux platforms. FoxTelem can decode telemetry stored as a wav file or acquired through the sound card and display the associated data frames. Slow speed data, or data under voice, transmits 200 bps data in the sub audible band of the transponder. Data are constructed as a 58 byte frame with a header. Real-time health is displayed in Figure 6. FoxTelem also simplifies the process to upload your telemetry to the AMSAT server and download the entire telemetry set. Each of the telemetry values can be plotted over time by clicking on the field. The temperature at the IHU computer, for instance, can be displayed as show in Figure 7.

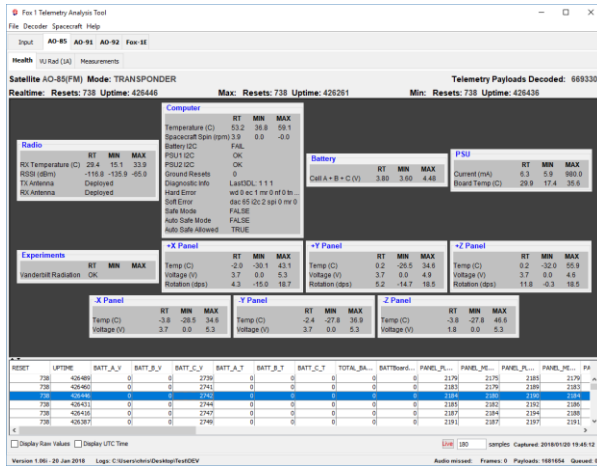


Figure 6: Fox Health shows real time telemetry

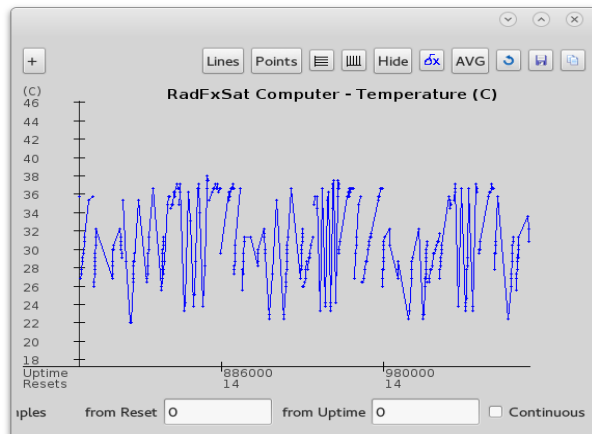


Figure 7: RadFxCsat computer temperature telemetry plotted in FoxTelem

Science data are also accessible through the FoxTelem interface. Each of the experiments returns a telemetry string when powered on and are presented in Figure 8. The top box indicates the number of microcontroller resets, the uptime of the microcontroller, current SRAM core voltage, and the cumulative SRAM livetime and bit errors.

All science data are based on telemetry collected by amateur radio operators and submitted through FoxTelem. The coordinates of the ground stations, for gauging participation only, can be placed by self-identified call signs on the AMSAT leaderboard and home station identified in the QRZ database.¹⁴ The map, shown in Figure 9, of course does not accurately account for unidentified contributors or mobile operators. Each marker indicates the number of frames reported on a logarithmic scale with red indicating the maximum at over 235,000.

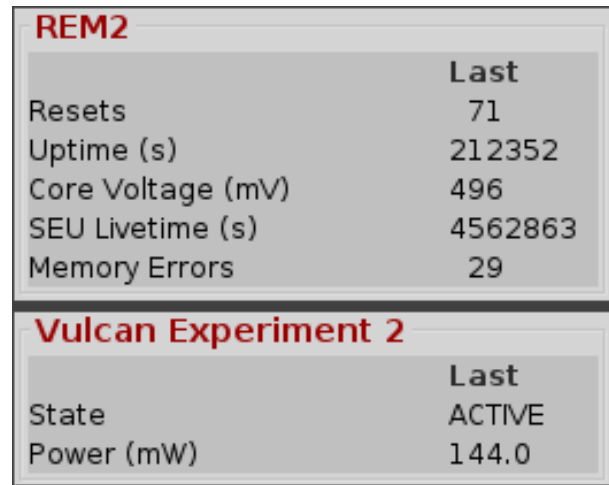


Figure 8: Experiment board real time telemetry in FoxTelem

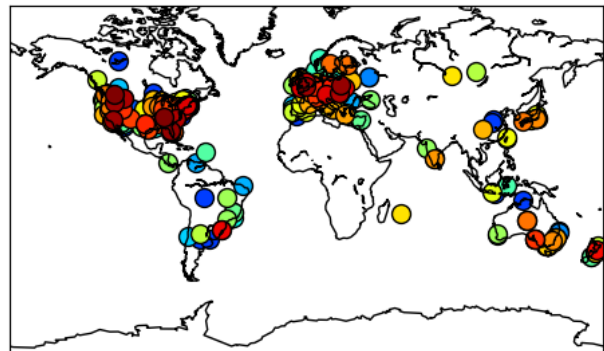


Figure 9: Location of amateur radio operator ground stations

ON-ORBIT SCIENCE DATA

18 months of telemetry have been collected since the launch of RadFxSat. The data provide a picture of the single event rate for bit errors. As described previously, the REM experiments report cumulative counts. Figure 10 plots the cumulative bit errors recorded by the experiment for each of the three REM boards. The interleaving of the data sets are a result of power cycling between boards. Periods without data at the beginning of the mission are a result of commissioning and a payload functional interrupt remedied in July 2018.

Typically, errors affect a single bit and are infrequent for the capacity of memory tested. However, REM3 recorded a large jump in errors at the end of March 2018. Plausible explanations include a particle strike to read/write peripheral circuitry or data corruption in the microcontroller. The event is doubly-suspect as the error count resumes at 64, a power of two. Focusing on the data collected after July 2018 provides a better sense of the frequency of bit errors.

The reduced counts in REM4 cannot be attributed to additional shielding as it was located at the top of the board stack. Rather, the SRAM core voltage on REM4 was held at 0.85 V instead of 0.5 V as was done on REM2 and REM3. This is qualitatively consistent with the bias dependence of ion-induced single event upset cross sections.¹⁵ The device error rate (upsets/hr) is derived as the ratio of errors to the experiment livetime. Table 2 summarizes the total values reported at the beginning of June 2019.

The RadFxSat mission was only one in a series of radiation effects studies enabled by CubeSats. Table 3 summarizes past and future launches. The goal of the program is not to qualify or even characterize candidate parts for spaceflight. Considering the unsubsidized cost of launch and development, on-orbit experiments do not

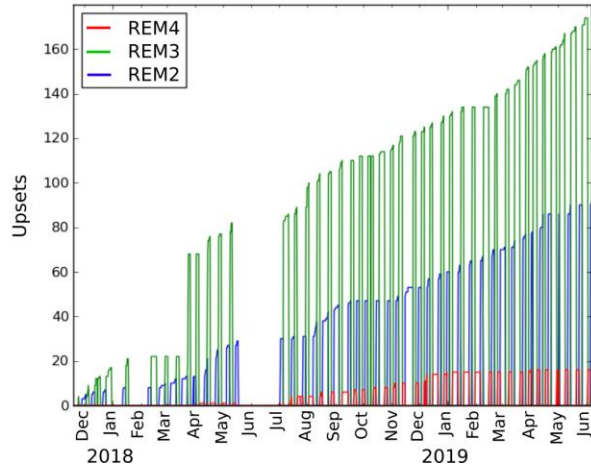


Figure 10: Cumulative bit errors reported in REM experiments

Table 2: Mission Averaged Error Rates

Board	Error Counts	Livetime (hr)	Normalized Error Rate
REM4	16	1265	0.013
REM3	132 [†]	4110	0.032
REM2	91	3781	0.024

[†] Adjusted for April 2018 anomaly

present a cheap alternative to ground-based test campaigns. Rather, the program is an effort to gather data to validate radiation hardness assurance approaches and models. In particular, we are interested in the continued effects of microelectronic scaling on the radiation reliability. The program has had three successful launches, but unfortunately Fox-1C suffered an anomaly with its radio and cannot be commanded. Future launches will investigate single event upsets in a highly-scaled FinFET process technology.

Table 3: RadFx Mission Summary

Design	Description	Status
Fox1-A	Investigates single event upsets in 8 identical 4Mbit commercially-available SRAMs	AO-85 launched Oct. 8, 2015 (completed 3 years operation)
Fox1-B	Investigates single event upsets across bias in 3 identical 28 nm commercial test chips.	AO-91 launched Nov. 18, 2017 (operational)
Fox1-C (Fox1-A flight spare)	Investigates single event upsets in 8 identical 4Mbit commercially-available SRAMs.	AO-95 launched Dec. 3, 2018 (communication failure)
Fox1-E	Investigates single event upsets across technology including 16nm FinFET SRAM	Planned launch Q3 2019
GOLF-TEE	Investigates single event upsets in 16nm FinFET SRAM	Planned launch 2020

Acknowledgments

The authors would like to acknowledge the late Anthony Monteiro, AA2TX, who served as the AMSAT VP of Engineering and established this collaboration with Vanderbilt University. In addition, the authors would like to express their gratitude for all the amateur radio operators that have collected and reported AO-91 telemetry. Special thanks to WA7FWF, WA4SCA, SQ5WAF, K4OZS, KB6LTY, N7DJX-DN13, G7WIQ, WC7V(dn46), N8MH, and OM3BC whose ground stations collected the most data frames as of the writing of this manuscript. Thanks to Broadcom Corporation for providing and supporting the memory under test. This work was supported by the Arnold Engineering Development Complex contract no FA9101-13-D-0002.

References

1. K. P. Rodbell et al., "Low-energy proton-induced single-event-upsets in 65 nm node, silicon-on-insulator, latches and memory cells," *IEEE Trans. Nucl. Sci.*, vol. 54, no. 6, pp. 2474–2479, Dec. 2007.
2. D. F. Heidel et al., "Low energy proton single-event-upset test results on 65 nm SOI SRAM," *IEEE Trans. Nucl. Sci.*, vol. 55, no. 6, pp. 3394–3400, Dec. 2008.
3. B. D. Sierawski et al., "Impact of low-energy proton induced upsets on test methods and rate predictions," *IEEE Trans. Nucl. Sci.*, vol. 56, no. 6, pp. 3085-3092, Dec 2009.
4. N. A. Dodds et al., "Hardness assurance for proton direct ionization-induced SEEs using a high-energy proton beam," *IEEE Trans. Nucl. Sci.*, vol. 61, no. 6, pp. 2904–2914, Dec. 2014.
5. J. A. Pellish et al., "Criticality of low-energy protons in single-event effects testing of highly-scaled technologies," *IEEE Trans. Nucl. Sci.*, vol. 61, no. 6, pp. 2896-2903, Dec 2014.
6. A. J. Tylka et al., "CREME96: A revision of the cosmic ray effects on micro-electronics code," *IEEE Trans. Nucl. Sci.*, vol. 44, no. 6, pp. 2150–2160, Dec. 1997.
7. B. D. Sierawski et al., "Cubesats and crowd-sourced monitoring for single event effects hardness assurance," *IEEE Trans. Nucl. Sci.*, vol. 64, no. 1, pp. 293-300, Jan 2017.
8. T. Monteiro, "AMSAT Fox Satellite Program," presented at AMSAT Space Symp., 2012.
9. R. A. Austin et al., "RadFxSat: A Flight Campaign for Recording Single-Event Effects in Commercial Off-the-Shelf Microelectronics," *2017 17th European Conf on Rad. and Its Effects on Components and Systems (RADECS)*, Geneva, Switzerland, 2017, pp. 1-5.
10. R. A. Austin et al., "A CubeSat-payload radiation-reliability assurance case using goal structuring notation," *2017 Annual Reliability and Maintainability Symposium (RAMS)*, Orlando, FL, 2017, pp. 1-8.
11. R. A. Austin, "A Radiation-Reliability Assurance Case using Goal Structuring Notation for a CubeSat Experiment," M.S. thesis, Vanderbilt University, Nashville, 2016.
12. National Aeronautics and Space Administration, NASA reliability and maintainability (R&M) standard for spaceflight and support systems, NASA-STD-8729.1A, Jun. 2016.
13. Radio Amateur Satellite Corporation, (June 2019) FoxTelem Software for Windows, Mac, and Linux. [Online]. Available: http://www.amsat.org/?page_id=4532.
14. QRZ. Callsign Database by QRZ, accessed on Jun. 29, 2016. [Online]. Available: <https://www.qrz.com/>
15. J. M. Trippe, "Monte Carlo methods for predicting SRAM vulnerability to muon and electron induced single event upsets," Ph.D. dissertation, Vanderbilt University, Nashville, 2018.